

# Interplay between RNA-binding protein HuR and Nox4 as a novel therapeutic target in diabetic kidney disease



Qian Shi<sup>1,\*</sup>, Doug-Yoon Lee<sup>2</sup>, Denis Féliers<sup>2</sup>, Hanna E. Abboud<sup>2,3</sup>, Manzoor A. Bhat<sup>1</sup>, Yves Gorin<sup>2,4</sup>

## ABSTRACT

**Objective:** Glomerular injury is a prominent pathological feature of diabetic kidney disease (DKD). Constitutively active NADPH oxidase 4 (Nox4) is a major source of reactive oxygen species that mediates hyperglycemia-induced mesangial cell (MC) fibrotic injury. However, the mechanism that Nox4 utilizes to achieve its biological outcome remains elusive, and the signaling pathways that regulate this isoform oxidase are not well understood. Here, our goal is to study the detailed mechanism by which NADPH oxidase 4 (Nox4) is post-transcriptionally regulated in MC during diabetic pathology.

**Methods:** We studied the protein expression of HuR, Nox4 and matrix proteins by western blotting, while we assessed the mRNA stability of Nox4 by RT-PCR and polysomal assay, examined *in vitro* cultured glomerular mesangial cells treated by high glucose (HG) and diabetic animal induced by STZ. The binding assay between HuR and the Nox4 promoter was done by immuno-precipitating with HuR antibody and detecting the presence of Nox4 mRNA, or by pull-down by using biotinylated labeled Nox4 promoter RNA and detecting the presence of the HuR protein. The binding was also confirmed in MCs where Nox4 promoter-containing luciferase constructs were transfected. ROS levels were measured with DHE/DCF dyes in cells, or lucigenin chemiluminescence for Nox enzymatic levels, or HPLC assay for superoxide. HuR protein was inhibited by antisense oligo that utilized osmotic pumps for continuous delivery in animal models. The H1bAc1 ratio was measured by an ELISA kit for mice.

**Results:** We demonstrate that in MCs, high glucose (HG) elicits a rapid upregulation of Nox4 protein via translational mechanisms. Nox4 mRNA 3' untranslated region (3'-UTR) contains numerous AU-rich elements (AREs) that are potential binding sites for the RNA-binding protein human antigen R (HuR). We show that HG promotes HuR activation/expression and that HuR is required for HG-induced Nox4 protein expression/mRNA translation, ROS generation, and subsequent MC fibrotic injury. Through a series of *in vitro* RNA-binding assays, we demonstrate that HuR acts via binding to AREs in Nox4 3'-UTR in response to HG. The *in vivo* relevance of these observations is confirmed by the findings that increased Nox4 is accompanied by the binding of HuR to Nox4 mRNA in kidneys from type 1 diabetic animals, and further suppressing HuR expression showed a reno-protective role in a type 1 diabetic mouse model via reducing MC injury, along with the improvement of hyperglycemia and renal function.

**Conclusions:** We established for the first time that HuR-mediated translational regulation of Nox4 contributes to the pathogenesis of fibrosis of the glomerular microvascular bed. Thus therapeutic interventions affecting the interplay between Nox4 and HuR could be exploited as valuable tools in designing treatments for DKD.

Published by Elsevier GmbH. This is an open access article under the CC BY-NC-ND license (<http://creativecommons.org/licenses/by-nc-nd/4.0/>).

**Keywords** NADPH oxidase 4; Human antigen R protein; Diabetic nephropathy; Translational regulation

## 1. INTRODUCTION

Diabetes is increasingly recognized as the leading cause of chronic renal failure, and a majority of the patients progress to end-stage renal disease (ESRD) requiring lifetime dialysis or kidney transplants [1,2]. Diabetic nephropathy (DN) is now clinically identified by progressively elevated protein albuminuria and a subsequent decline in glomerular filtration rate [3]. A predetermined course usually preceded by the pathogenesis and clinical manifestations of DN is viewed as marked

structural alternations in the kidney, including renal hypertrophy, enlarged glomerular capillaries, mesangial expansion, and thickening of the glomerular basement membrane. Extracellular matrix expansion in glomeruli contributes to the pathogenesis of those hallmarks [4]. Data from diabetic animal models showed that hyperglycemia and high glucose (HG) significantly enhance extracellular matrix accumulation in mesangial cells.

Reactive oxidative species (ROS) has emerged as a critical pathogenic factor in the pathological development of renal and other vascular

<sup>1</sup>Department of Cellular and Integrative Physiology, The University of Texas Health Science Center at San Antonio, San Antonio, TX 78229, USA <sup>2</sup>Department of Medicine/ Division of Nephrology, Long School of Medicine, The University of Texas Health Science Center at San Antonio, San Antonio, TX 78229, USA

<sup>3</sup> Deceased on January 7, 2015.

<sup>4</sup> Deceased on August 28, 2018.

\*Corresponding author. Department of Cellular and Integrative Physiology, University of Texas Health Science Center, 7703 Floyd Curl Drive, San Antonio TX 78229-3900, USA. E-mail: [shiq@uthscsa.edu](mailto:shiq@uthscsa.edu) (Q. Shi).

Received December 15, 2019 • Revision received February 14, 2020 • Accepted February 22, 2020 • Available online 28 February 2020

<https://doi.org/10.1016/j.molmet.2020.02.011>

diseases, particularly in DN [5–7]. Identifying sources of ROS should help design optimized treatments to modulate oxidative stress in a tissue-specific manner or under unique pathological conditions. Major sources of ROS in various organs/cells are identified as NADPH oxidases (Nox), the only family of enzymes dedicated to generating ROS [8]. Seven Nox proteins have been identified in the human genome: Nox1–5 and the dual oxidases Duox1 and 2. In the kidney, the major isoform Nox4 is responsible for generating ROS and is involved in the damaging effects of HG that significantly contribute to microvascular complications associated with diabetes [7]. We have previously reported that Nox4-dependent ROS mediates glomerular hypertrophy and mesangial matrix accumulation in type 1 diabetic mouse models. In mesangial cells, those Nox4-derived ROS lead to elevated fibronectin protein expression when exposed to HG [9]. However, the mechanism that Nox4 utilizes to exhibit its biological outcome remains elusive, and the signaling pathways that regulate this oxidase isoform are also not well understood.

In a recent study by Yu et al. [10], the additional role of an RNA regulating/binding protein, HuR, has been found in the pathogenesis of DN, suggesting protein HuR may promote the Epithelial–mesenchymal transition (EMT) process in diabetic kidney complications and contribute to the matrix accumulation in tubular epithelial cells when exposed to HG. Here, we provided a detailed mechanistic analysis underlining HuR-mediated, HG-induced elevation of ROS and matrix protein accumulation in kidney mesangial cells. We found that HuR can bind to 3′-UTR of Nox4 and mediate its mRNA stability, and thus affect its translational efficiency. We established for the first time that HuR-mediated translational regulation of Nox4 contributes to the pathogenesis of fibrosis of the glomerular microvascular bed, potentially through increased ROS production. The current study provides the foundation for future research focusing on the dual inhibition of Nox4 and HuR as a potential therapeutic option for treating DN.

## 2. RESEARCH DESIGN AND METHODS

### 2.1. Cell culture and HG treatment

Glomerular mesangial cells were isolated from rat kidneys and characterized as described previously [11]. The cells used in the current study were maintained between the 15th and 30th passages from the initial culture, in high glucose DMEM supplemented with antibiotic/antifungal solution and 17% fetal bovine serum. MCs grown to 80–90% confluence were serum-deprived for 48 hours and exposed to serum-free DMEM containing 5 mM D-glucose or 25 mM D-glucose for the duration specified in the text.

### 2.2. Human tissue samples

Human kidney tissues from patients with diabetic nephropathy and healthy human kidney tissues were obtained from NIDDK Tissue Bank for Developmental Disorders at the University of Maryland, Baltimore, MD. All human tissues were obtained in accordance with a protocol approved by the UT Health Science Center at the San Antonio Institute Review Board and Committee on Human Research.

### 2.3. Plasmids, transfection, and infection

Control siRNA (sc-37007) and pools of siRNAs against HuR (sc-270446) were purchased from Santa Cruz Biotechnology (Santa Cruz, CA). siRNA transfection was performed using an oligofectamine reagent (Invitrogen) with an OPTI-MEM serum-free medium (Invitrogen), according to the manufacturer's instructions. The suppression of protein expression was analyzed by immunoblotting.

An hLuc/Rluc plasmid, pEZX-MT01, containing wild type human Nox4 3′-UTR (UTR length: 2.4 kb, cat#HmiT054569-MT01) was purchased from GeneCopoeia (Rockville, MD). To generate the mutants on AREs that disrupt the potential binding region for HuR, we performed the site-directed mutagenesis with the primers listed in the [Supplementary Table 2](#), and the experimental protocols were followed according to the manufacturer's protocol (Q5 Site-Directed Mutagenesis Kit, NEB). All sequences of mutants were verified by sequencing at the UTHSCSA core facility.

### 2.4. Dual luciferase assay

Dual luciferase assays were performed with the dual luciferase reporter assay system (GeneCopoeia, Rockville, MD). All reagents were prepared as described by the manufacturer. Luminescence measurements were performed with a Promega GLOMAX 20/20 luminometer (Promega Corp., Madison, WI). The data are represented as the ratio of firefly to *Renilla* luciferase activity (Fluc/Rluc).

### 2.5. Polysome assay

The polysome assay was performed as described [12]. Briefly, post-nuclear supernatants were separated on a 15–40% sucrose gradient by centrifugation at 200,000 × g and divided into 10 fractions. Total RNA was isolated by the TRIzol method and used for quantitative RT-PCR.

### 2.6. Immunoblotting and antibodies

Cells or tissues were collected/homogenized and lysed on ice in an RIPA buffer (25 mM Tris–HCl, pH 7.5, 150 mM NaCl, 1 mM EDTA, 1% NP-40 and 5% glycerol) with protease inhibitors (#88660SPCL, Thermo Fisher Scientific) and a phosphatase inhibitor mix (sc-45044, Santa Cruz). Immunoblotting was performed by probing with the following antibodies: anti-Nox4 (sc-30141), anti-Lamin (sc-376248) and anti-HuR (sc-5261) from Santa Cruz; monoclonal anti-GAPDH (G8795) from Sigma; and anti-fibronectin (ab2413) and anti-SMA (ab5694) from Abcam.

### 2.7. RNA extraction and RT-PCR analyses

Total RNA from cells or tissues was isolated by using the PureLink™ RNA mini kit (Ambion). cDNA reverse transcription was performed with the High Capacity cDNA Reverse Transcription kit (Applied Bio System), and the amplified product was separated by agarose gel electrophoresis. Quantitative RT-PCR was performed with SYBR green PCR Master Mix (Applied Bio System) on the Eppendorf Realplex Real-Time PCR System, and primers were used as previously reported [13].

### 2.8. Measurement of mRNA half-life

The half-life of Nox4 mRNA was determined using actinomycin D as described previously [13]. The quantity of Nox4 mRNA was first normalized to the amount of 18 S rRNA by calculating a Nox4:18 S ratio for each sample, and then was normalized to groups without actinomycin D treatment. The data are expressed as the percentage of mRNA molecules before the actinomycin D treatment.

### 2.9. Ribonucleoprotein (RNP) IP assays

For assessment of the association of endogenous HuR with endogenous Nox4 mRNA, immunoprecipitation of RNP complexes was performed. Briefly, 20 × 10<sup>6</sup> cells were collected per sample, and lysates were prepared for IP for overnight at 4°C in the presence of a 25 μg HuR antibody, or an equal amount of IgG1 as a negative control. RNA in the IP complex was collected on beads and subjected to cDNA synthesis

and RT-qPCR analyses to detect the presence of Nox4 and GAPDH mRNAs.

#### 2.10. Biotin-RNA pull-down assays

To verify the association between HuR and Nox4 3'-UTR, biotinylated RNAs were synthesized at IDT (Coralville, IA), and 6  $\mu$ g of RNA was incubated with designed cell lysates (100  $\mu$ g total protein) for 2 h at room temperature. RNA-protein complexes were then isolated with paramagnetic streptavidin-conjugated Dynabeads (Dyna, Oslo, Norway) and analyzed by western blotting assay. Antibodies against HuR or control IgG was added in certain groups for the competition assay. Mutated biotinylated RNA molecules were also generated and subjected to similar experiments. All sequences of RNA are summarized in the [Supplementary Table 1](#).

#### 2.11. Measurement of oxidative species by DHE (dihydroethidium) and DCF (2',7'-dichlorodihydrofluorescein diacetate) staining

For staining, rat MCs cells were seeded in 4-chamber slides. After designated treatments, the cells were briefly washed with PBS and incubated in 1  $\mu$ M DHE (#D1168 ThermoFisher) or DCF dye (#D399, ThermoFisher) for 30 min. Then, the cells were quickly washed with PBS 3 times and fixed in 4% paraformaldehyde for 30 min at room temperature. After fixation, cells were washed again 3 times and immediately subjected to confocal microscopy imaging. Representative fluorescent images from random regions were taken and the fluorescence signals were determined using ImageJ software. DAPI was used as counter-staining for nuclei.

#### 2.12. Measurement of NADPH oxidase activity by lucigenin chemiluminescence assay

NADPH oxidase activity was measured in cells grown in the serum-free medium or in the kidney cortex isolated from rats or mice as previously described [13,14]. Briefly, 20  $\mu$ g of homogenates were added to the assay buffer (50 mM phosphate buffer, pH 7.0, containing 1 mM EGTA, 150 mM sucrose) with 5  $\mu$ M lucigenin and 100  $\mu$ M NADPH. Photon emission expressed as relative light units was measured every 30 s for 10 min in a luminometer. Superoxide production was expressed as relative light units per milligram of protein.

#### 2.13. HPLC analysis of superoxide

Superoxide production *in vivo* or in HRP cells were assessed by HPLC analysis of the DHE-derived oxidation products, as reported previously [15,16]. This assay allows segregation of superoxide-specific EOH from the nonspecific ethidium. Chromatographic separation was carried out with the use of a NovaPak C18 column in a HPLC system (LC-2000 plus series; Jasco Inc., Easton, MD).

#### 2.14. Immunohistochemical immunofluorescence staining

The localization of Collagen IV (1:200, ab214417, Abcam), Nox4 (1:200, Santa Cruz), and HuR (1:200, Santa Cruz) was assessed in paraffin-embedded sections (5  $\mu$ m thick) by alkaline phosphatase histochemistry. The glomerular tuft area and mesangial matrix expansion were evaluated using the Image-Pro plus software, as described before [16,17].

#### 2.15. Induction of type-1 diabetes in mice and rat

Diabetes was induced in 8-week-old male C57BL/6 mice (body weight between 21 and 26 g) or rats (body weight between 200 and 250 g), with the five daily low dose protocol as described previously [9], via i.p. injections of streptozotocin (Sigma—Aldrich, St Louis, MO, USA) (50 mg/kg) for mice, or tail vein injection for rats (55 mg/kg).

Only mice with blood glucose  $\geq$ 15 mmol/L after injection of streptozotocin have been included in the experiments (>80% of the total number of mice).

#### 2.16. Inhibiting HuR protein in mice by antisense oligonucleotides

Phosphorothioated sense (S) (5'-AAC AUG ACC CAG GAU GAG UUA-3') or antisense (AS) (5'-UAA CUC AUC CUG GGU CAU GUU-3') oligonucleotides for HuR were synthesized by IDT Inc. and then injected to mice following an STZ induction (90 ng/g of body weight/day) by an Alzet osmotic pump for a continuous 14 days (ALZA, Palo Alto, CA) as previously described [9,13].

#### 2.17. Blood glucose and glycated hemoglobin (HbA1c) measurement

Blood glucose levels were measured 2–3 times every week, using an Accu-Chek glucometer (Roche Diagnostics) following a 4–6 h fasting period. Glycated hemoglobin A1c (HbA1c) was measured using an ELISA kit (Cat# E4657-100, BioVision, Milpitas, CA). Briefly, mouse blood was collected, and plasma were separated by centrifugation at 1000 $\times$ g at 4  $^{\circ}$ C. The supernatant was collected and subjected to the assay immediately. The experiment was performed accordingly to the manufacture's protocols and the results were read at 450 nm.

#### 2.18. Renal function measurement

The urinary protein albumin was measured after collecting urine for 24 hours while mice were kept in a metabolic cage. Urine albumin levels were determined using a murine microalbuminuria ELISA kit (Exocell, Inc., Philadelphia, PA).

#### 2.19. Statistical analysis

Data are presented as means  $\pm$  SE. Statistical analysis between multiple groups was performed by one-way ANOVA (nonparametric), and post-test analysis was performed using Tukey Statistical by GraphPad Prism software. A *p* value of 0.05 or less was considered statistically significant.

### 3. RESULTS

#### 3.1. High glucose (HG) upregulates Nox4 protein expression acutely in glomerular mesangial cells (MCs) and induces nuclei-cytoplasm shuttling

In the histological features of diabetic nephropathy, the glomerular capillary network shows hypertrophy and matrix expansion, in which mesangial cells go through metabolic and hemodynamic changes and help maintain the homeostasis of the mesangial matrix by releasing soluble molecules. We utilized rat mesangial cells for our analysis and examined the effects of HG (25 mM D-glucose) on these cells, or normal glucose (5 mM D-glucose) after 48 hours of serum deprivation. Acute exposure to HG stimulated the expression of Nox4 protein (Figure 1A); however, the elevated protein levels of Nox4 were not correlated with levels of Nox4 mRNA (data not shown). As we showed a similar observation in human kidney epithelial cells with the dysregulated mTOR signaling pathway [13], we decided to examine the mechanisms underlying Nox4 protein expression.

Maintaining mRNA stability is one of the mechanisms involved in enhanced translational efficiency. HuR is one of the most well-characterized RNA-binding proteins that stabilizes different mRNAs by binding to AU-rich elements located in 3'-UTR. The total amount of HuR inside the cells showed acute increase after HG treatment, measured by western blotting assay (Figure 1A). More importantly,

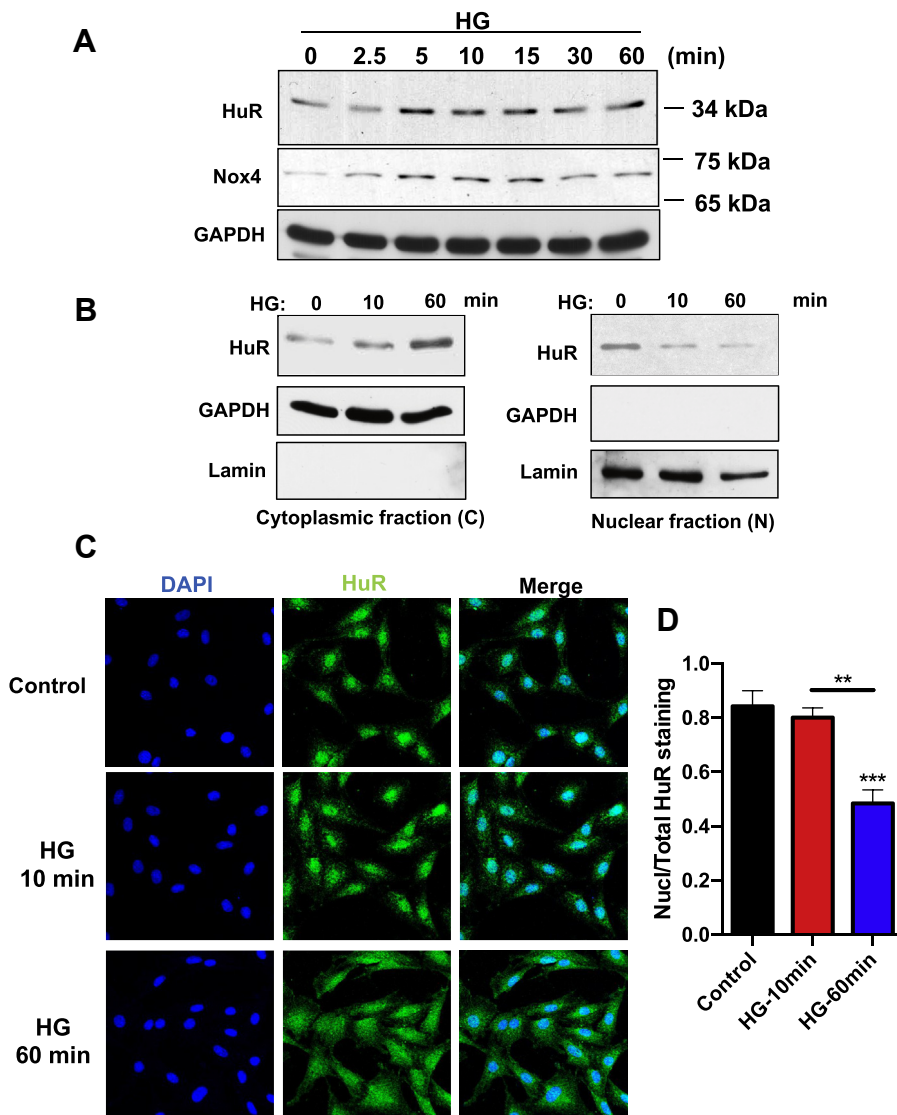


**Figure 1:** High glucose (HG) upregulates HuR protein expression acutely in glomerular mesangial cells (MCs), and induces its cytoplasmic-nuclear shuttling. (A) HuR and Nox4 protein levels in MCs after exposure to HG for various time points, measured by immunoblotting assay. GAPDH was served as loading control. (B) HuR protein expression in cytoplasmic and nuclear fraction of MCs, after exposure to HG for 10 and 60 min. GAPDH was used as control for cytoplasmic fraction, and Lamin was used here for nuclear fraction. (C) Immunofluorescence detection of HuR in MC cells after exposing to HG for 10 or 60 min. DAPI staining was used to localize nuclei. Pictures are representative of three separate experiments (scale bar, 20  $\mu$ m). All images were observed and analyzed under a confocal laser-scanning microscope (Fluoview; Olympus Optical, Tokyo, Japan). (D) Intensity of immunofluorescence was measured by Image J software and presented as the ratio of Nuclear staining over total staining. All data are presented as the mean  $\pm$  S.E. of three repeats. \*,  $p < 0.05$ ; \*\*,  $p < 0.01$  in comparison with control or as indicated. Student's  $t$ -test was used to compare two groups; and one-way ANOVA was used for comparison between multiple groups.

consistent with Nox4 activation, short term treatment of MCs with HG significantly boosted the nuclei-cytoplasm translocation of HuR. Cellular fraction experiments suggested that HuR proteins were enriched in the cytosol and gradually decreased in nuclear fractions after HG stimulation (Figure 1B). Such nuclei-cytoplasmic shuttling was confirmed with immunofluorescence experiments. Cells were labeled with HuR antibody (green), and HuR signaling quickly shifted to cytosol from nuclei starting at 10 min and peaking at 1 h (Figure 1C). The quantification of HuR nuclear translocation is shown in Figure 1D. Taken together, these data suggested that HG can induce the translocation of HuR from nuclei to cytosol and lead to the activation of HuR, which could potentially be involved in regulating the mRNA stability of Nox4.

### 3.2. HuR is required for HG-induced Nox4/ROS increase, MCs fibrotic injury and the maintenance of Nox4 mRNA stability

Given the growing body of evidence showing that HuR translocation to the cytoplasm is linked with its ability to stabilize target mRNAs, we sought to determine whether HuR is required for increased Nox4 mRNA translation efficiency. The increased level of Nox4 protein upon HG stimulation was significantly abolished when cells were pre-treated with HuR siRNAs (Figure 2A). On the other hand, overexpression of HuR in MCs promoted the expression of Nox4, even without HG treatment (Figure 2B), suggesting that HuR plays an essential role in regulating Nox4 protein expression, most likely through binding to Nox4 mRNA. Since NADPH oxidases are known to generate ROS in kidney cells, we performed a lucigenin chemiluminescence assay (Figure 2C) combined

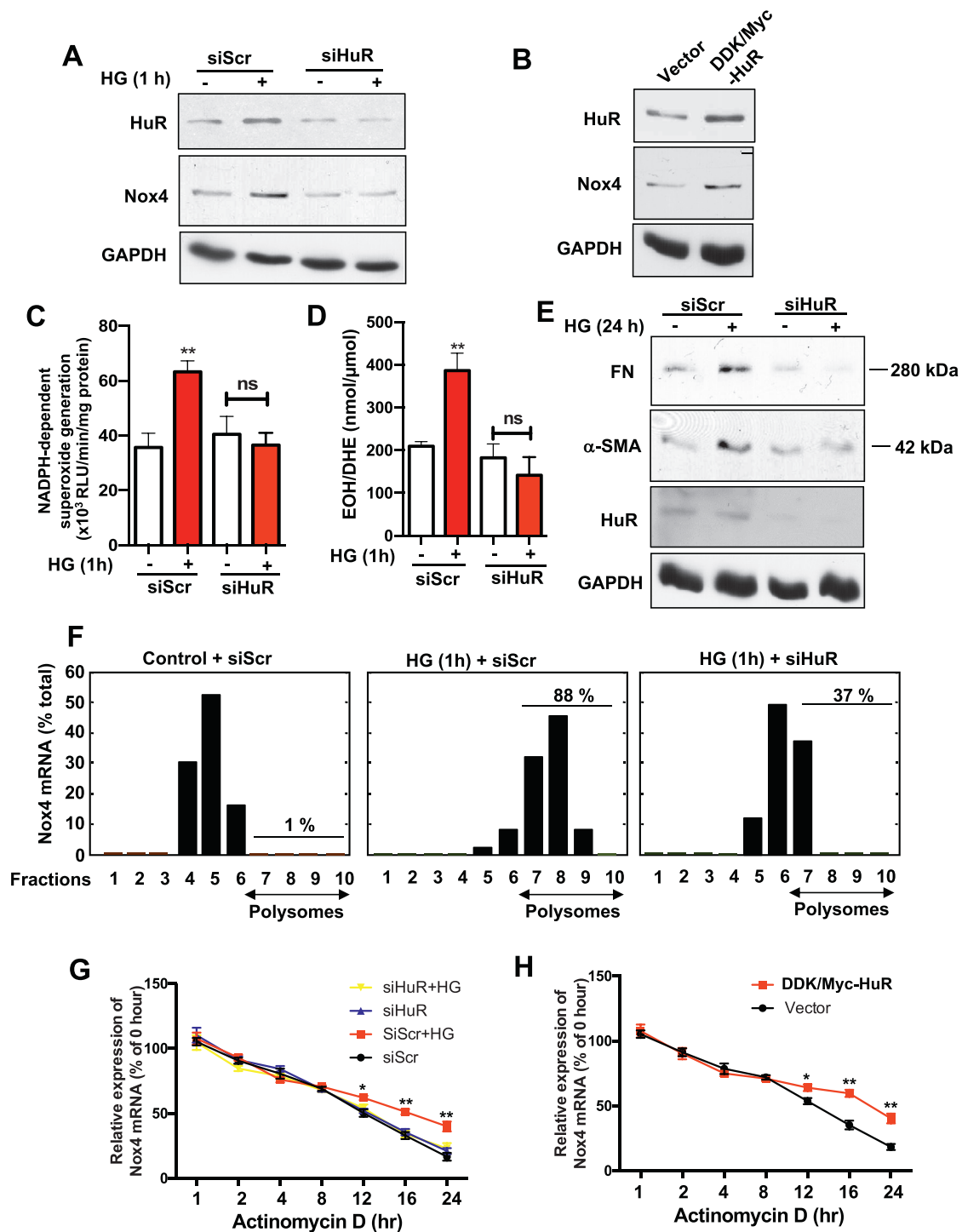


**Figure 2:** HuR is required for HG-induced Nox4/ROS increase, MCs injury and maintains Nox4 mRNA stability. (A) HuR and Nox4 protein levels in cells with scramble or siRNA against HuR along with HG exposure for 1 hour. Cells were treated with HG for 1 h before being subjected to cell lysis. GAPDH was used as a loading control. (B) HuR and Nox4 protein levels in MC cells with overexpression of Myc-HuR, by standard Lipofactmine 2000 transient transfection. (C, D) Nox activity (superoxide production) was measured in MC cells with scramble or siRNA against HuR after HG exposure for 1 h by lucigenin chemiluminescence (C) and HPLC assay (D) in designed cells. The data are presented as the mean  $\pm$  S.E of three repeats. \*\*,  $p < 0.01$  in comparison with cells receiving scramble siRNA and no HG treatment. (E) Fibronectin (FN) and  $\alpha$ -smooth muscle actin (SMA) were measured in MCs with siRNA against HuR by western blotting. (F) Polysomes assays were performed in MCs. Nox4 mRNA was measured with Taqman probes and presented here as the percentage in each fraction. (G, H) Nox4 RNA stability was measured by qRT-PCR after MCs were exposed to Actinomycin D (AcD) (5  $\mu$ g/mL), with control or HG, scramble or siRNA against HuR (G), and MCs with HuR overexpression construct or control vector (H). The data are expressed as the percentage of mRNA molecules before the actinomycin D treatment.

with HPLC—DHE (Figure 2D) methods to measure the enzymatic activity of Nox proteins, which generate superoxide. Nox enzymatic activity was significantly higher in the HG-treated MCs, and such an increase was abolished by the transfected HuR siRNA (Figure 2C,D). The total ROS levels in these cells were also measured by oxidant-sensitive dye H2DCFAD, which showed that ROS levels were significantly decreased in HuR knockdown cells when cells were treated with HG. This observation was confirmed by DHE, another cell-permeable ROS-sensitive probe (Supplementary Figure 1). Taken together, these results showed that reducing HuR protein levels significantly abolished the increased levels of ROS induced by HG treatment.

Mesangial cell hypertrophy is an important disease-promoting pathway in the progression of diabetic nephropathy and other glomerular diseases, which is also tightly associated with matrix protein accumulation. Indeed, we observed that the levels of fibronectin (FN) and  $\alpha$ -smooth muscle actin ( $\alpha$ -SMA), two markers for renal fibrotic injury, were increased with HG treatment in MCs; while silencing HuR mRNA significantly blocked the elevated expression of both FN and  $\alpha$ -SMA (Figure 2E). In summary, hyperglycemia enhanced Nox4 protein expression by promoting the binding of HuR to Nox4 3'-UTR, which leads to increased ROS levels followed by matrix protein accumulation.

mRNA structural modeling of the 3'-UTR of Nox4 showed that it harbors two stem-loop structures (data not shown). Such secondary stem-loop structures render mRNAs to be regulated by translation; for example, ribosomal proteins RPL23, RPL34, cyclin D1 and osteopontin [18]. Next, we further explored the mechanism in which HuR protein regulates the Nox4 mRNA translation by performing a polysome profiling assay. Data are expressed as the percentage of Nox4 mRNA measured in all fractions. Whereas in untreated MCs, only 1% of Nox4 mRNA was associated with polysomal fractions, the proportion was significantly increased to 88% in HG-treated MCs. While upon HuR-silenced cells, the abundance of Nox4 mRNA in the polysomal fraction decreased to 37% after HG 1-hour stimulation (Figure 2F). This further supported the hypothesis that HuR regulates Nox4 by regulating its mRNA translation efficiency. Such mechanistic regulation is normally associated with changes in mRNA stability. Nox4 mRNA levels were measured in the MCs treated with scramble siRNA or HuR siRNA upon HG stimulation after actinomycin D treatment. HG treatment did not enhance the total level of Nox4 mRNA (data not shown), but the half-life of Nox4 mRNA in HG-treated cells was significantly longer than in the control cells; the inhibition of HuR protein before HG treatment remarkably decreased the half-life of Nox4 mRNA as compared to the control levels (Figure 2G). However, the over-expression of HuR in MCs prolonged the half-life of Nox4 mRNA (Figure 2H). Taken together, our data reveal that HG-induced Nox4 protein up-regulation is HuR-dependent, and that depletion of HuR significantly abolished the HG-induced Nox4 protein increase, diminished the overall generation of ROS, and subsequently decreased the matrix protein accumulation.

### 3.3. HuR specifically binds to the Nox4 3'-UTR, and this binding increases after HG treatment

To further study how HuR binds to Nox4 mRNA and regulates its mRNA stability at the molecular level, we sought to confirm the physical binding between Nox4 mRNA and HuR protein in RNA pull-down experiments. As shown in Figure 3A, Nox4 mRNA was present in the complex immunoprecipitated with an HuR antibody; but the Nox4 mRNA level was undetected in the IgG controls. Interestingly, the abundance of Nox4 mRNA in this complex was increased in response to HG treatment, suggesting that HG significantly

promoted the binding between Nox4 mRNA and HuR protein (Figure 3A).

It is well-characterized that HuR stabilizes its mRNA targets through direct binding to their specific *cis*-acting elements in the 3'-UTRs. Utilizing online bioinformatic tools (AREsite2), we identified several potential AREs (AUUUA motifs embedded in a larger U-rich context) in the 3'-UTR of Nox4 (Supplementary Figure 2), which prompted us to confirm the existence of a Nox4 mRNA—HuR complex in MCs with or without HG stimulation. To analyze such binding, we generated biotin-labeled short RNA sequences that were corresponding to the ARE regions in Nox4 mRNA 3'-UTR, and then analyzed the streptavidin beads complex incubated with cell lysates. HuR protein was detected in the lysate immunoprecipitated with both biotinylated RNAs (arrow, Lane 2 in Figure 3B), and the abundance of protein increased when cells were exposed to 1-hour HG treatment (Lane 3 in Figure 3B). Interestingly, the abundance of HuR protein was significantly reduced when an anti-HuR antibody was added in cell lysate before mixing with biotinylated RNA (Lane 4 in Figure 3B), further confirming the specific binding between HuR protein and Nox4 3'-UTR. To validate the specificity of these ARE sequences, we generated short RNA sequences that contain the point mutations (AUUUA to ACGCA), which disrupted the conserved HuR binding regions (see Supplementary Table 1 for all sequences for both wild-type and mutants). The HuR protein was found to be present in the complex with any of three tested wild type RNAs, and binding affinity was increased when cells were treated with HG. However, when incubated with mutated RNAs, the binding between HuR protein and mutated RNAs was not detected (Figure 3C), further confirming the specificity of binding between HuR and Nox4 3'-UTR mRNA.

Next, we examined this binding utilizing an *in vitro* cellular reporter system. We obtained a luciferase reporter construct (pEZX-MT01 from GeneCopoeia) containing 3'-UTR of Nox4. This plasmid construct was transiently transfected into MCs. Our results demonstrated the HG treatment resulted in increased activity of luciferase reporter signals compared to the controls (Figure 3D). The increased luciferase activity by HG treatment was significantly reduced by HuR siRNA (Figure 3E). To confirm that these ARE elements in 3'-UTR of the Nox4 mRNA were responsible for the observed effects, we disrupted all these AU-rich elements individually in 3'-UTR by introducing point mutations (Supplementary Figure 3). The results demonstrated that mutating any of these AREs abolished the 3'-UTR-mediated up-regulation of the luciferase reporter activity (Figure 3F). Here we concluded that the effects of the 3'-UTR of Nox4 mRNA on the expression of the luciferase reporter could be attributed to these ARE elements, likely through decreased mRNA binding to HuR protein. Therefore the increased binding between Nox4 mRNA and HuR protein was due to the presence of the AU-rich elements in the 3'-UTR of Nox4 mRNA.

### 3.4. The binding of HuR to Nox4 mRNA is increased in the kidneys from type 1 diabetic animals

To study the correlation between HuR protein and Nox4 mRNA *in vivo*, we induced type-1 diabetes in mice by injecting streptozotocin (STZ). Ten weeks after the initial 5-day injection, 80% of mice became diabetic (glucose concentrations were higher than 30 mg/L). Western blot showed that the protein levels of Nox4 in diabetic mouse kidneys were increased, as well the protein levels of HuR protein (Figure 4A). Also, the immunochemical analysis showed that the levels of HuR protein were increased in diabetic animals compared to the control group, especially concentrated in the glomerular area (Figure 4B, right panel for quantification). HuR protein was also found to increase in kidneys from OVE26 mice, which is a well-established type-1 diabetic

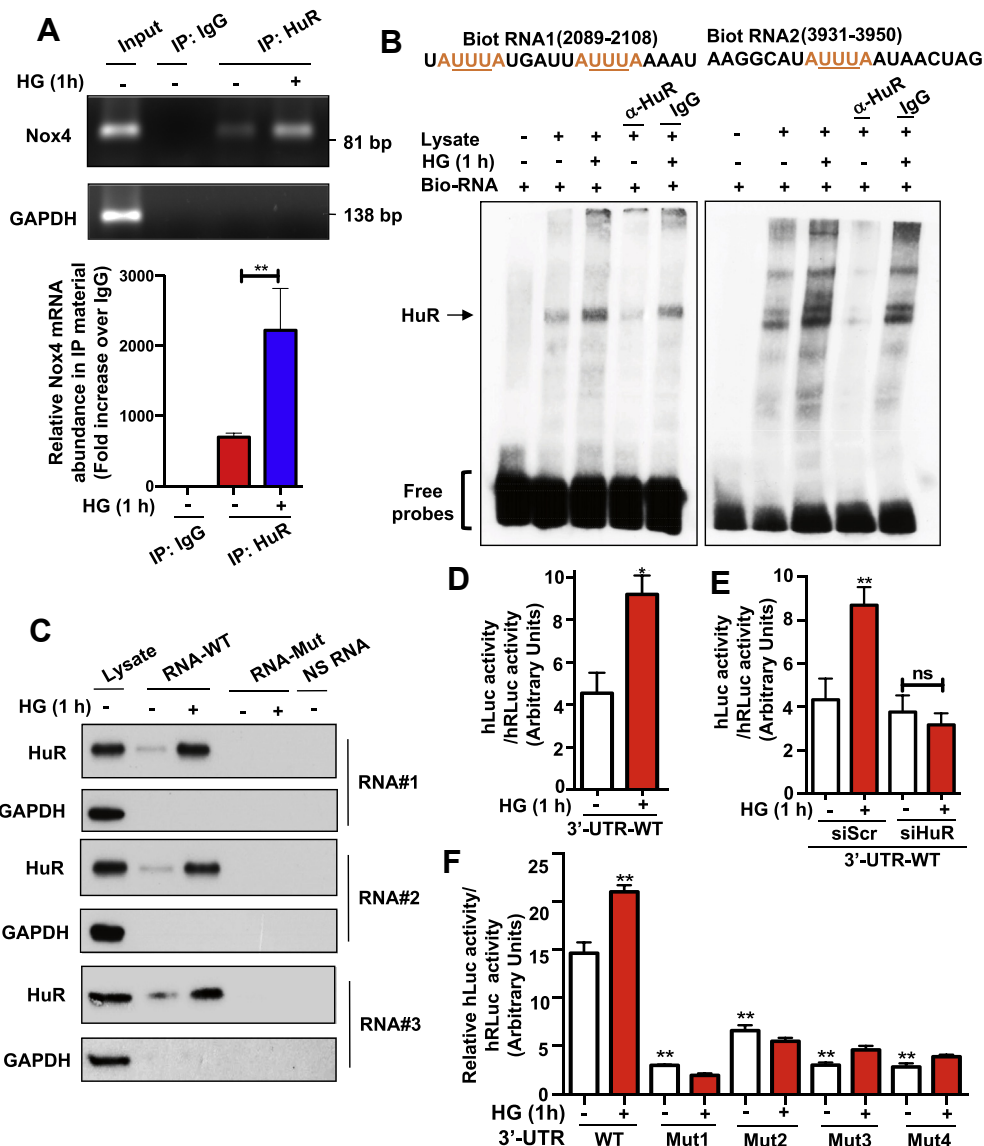


**Figure 3:** Transcripts encompassing the Nox4 3'-UTR associate with HuR protein and the abundance of the complexes increased in HG-treated MCs. (A) Nox4 mRNA was presented in the immunoprecipitants with HuR antibody in MCs, and its affinity was increased when cells were exposed to HG. Standard IP protocol was followed. Nox4 mRNA was detected by RT-PCR (upper panel) and quantified against the trace amount presented in total IgG complex (bottom panel). GAPDH served as a control. (B) Nox4 promoter containing AREs motifs were associated with HuR protein. RNA probes were synthesized with biotinylating labeling and incubated with MCs in the presence or absence of the HuR antibody. The RNA EMSA experiments were performed following the LightShift Chemiluminescent RNA EMSA Kit from ThermoSci Inc. (C) HuR protein was presented in RNA pull-down complex with wild type Nox4 promoter RNAs but not with mutated Nox4 promoter RNAs. Mutations were generated on ARE motifs located within Nox4 promoter RNAs. NS-RNA were random, non-specific binding RNAs that were used as negative controls. RNA pull-down complex was probed with the HuR antibody. (D–F) MCs were transiently transfected with a pEZ-MT02-hNox4 3'-UTR construct, a luciferase reporter construct containing human Nox4 3'-UTR region, and luciferase activity was recorded in various conditions. HG increased the luciferase reporter activity in MCs that were transiently transfected with this construct (D). Such effects were reduced by co-transfection with siRNA against HuR in HG-treated MCs (E). Mutation on ARE regions of Nox4 3'-UTR within pEZ-MT02-hNox4 3'-UTR construct disrupted the increased luciferase activity in MCs that were treated with HG (F). All data are presented as the mean  $\pm$  S.E of three repeats. \*,  $p < 0.05$ ; \*\*,  $p < 0.01$  in comparison with control or as indicated. The Student's *t*-test was used to compare the two groups; and one-way ANOVA was used for comparison between multiple groups.

mouse model (Figure 4C), further suggesting an important role of HuR in diabetic animals.

To confirm the binding between Nox4 mRNA and HuR protein *in vivo*, the kidneys from diabetic mice were subjected to an immunoprecipitation assay. The Nox4 mRNA was detected in the immunoprecipitated complex with HuR antibody, while it was absent in the controls with total rabbit IgG. In the kidneys from STZ-induced diabetic mice, the levels of Nox4 mRNA present in the IP complex was significantly increased (Figure 4D, bottom panel for quantification), suggesting that

hyperglycemia in mice also leads to the increased binding affinity between Nox4 mRNA and HuR protein. In STZ-injected rat diabetic models, rat Nox4 mRNA was also present in the IP complex with HuR antibody, and its abundance was enriched in the diabetic rat kidney (Supplementary Figure 4). More importantly, by examining paraffin-embedded sections of human kidney tissues, we found that the levels of HuR protein were dramatically elevated in kidney glomeruli from patients with diabetic nephropathy, as compared to the healthy/nondiabetic control subjects (Figure 4E). The intensity of glomerular HuR

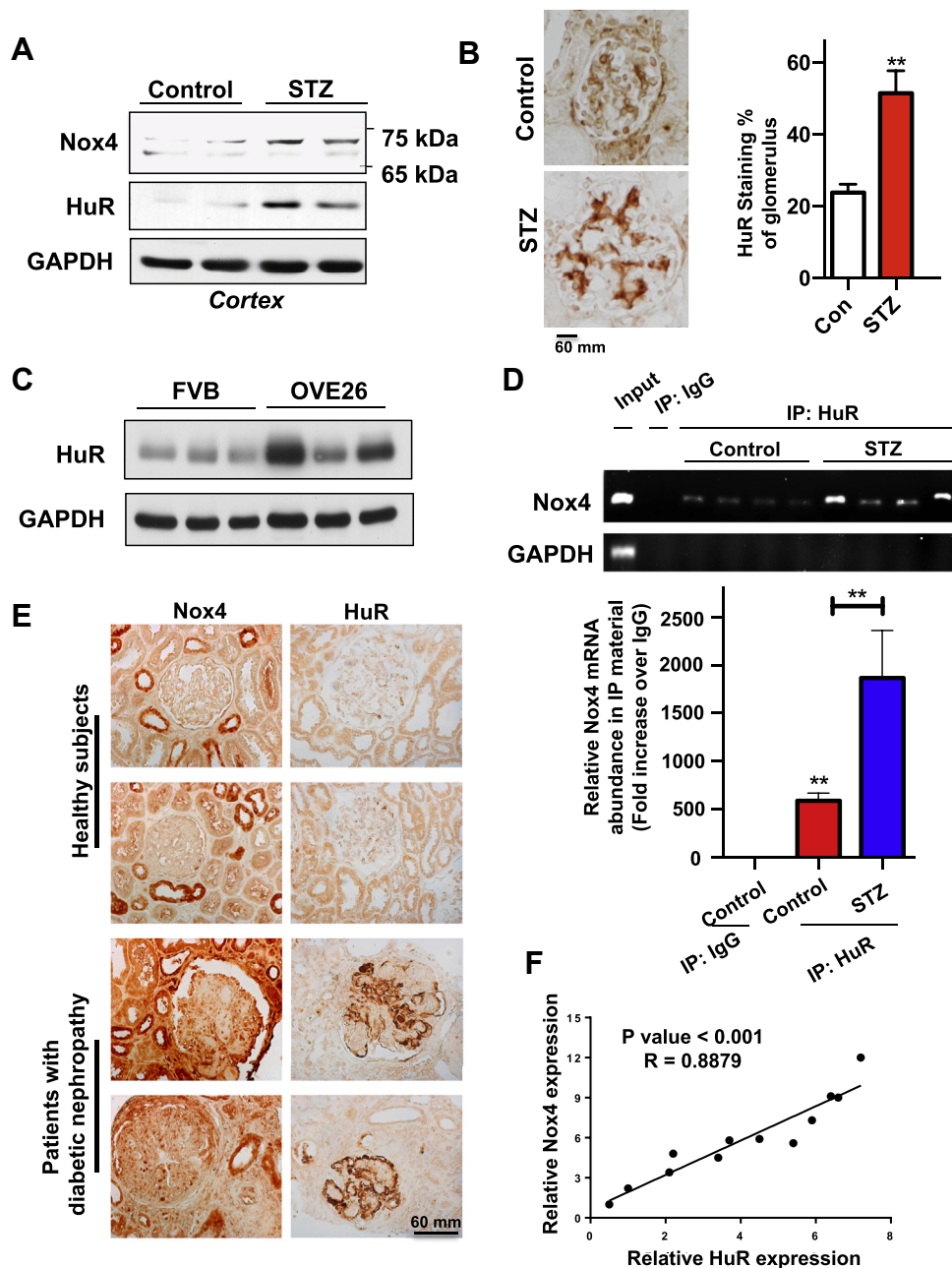


**Figure 4:** The binding of HuR to Nox4 mRNA is increased in kidneys from type 1 diabetic animals. (A) HuR and Nox4 protein levels were increased in kidneys from STZ-induced mice. Kidneys from control and STZ-induced mice were isolated and total protein was subjected to western blot, and GAPDH was used as a loading control. Representative images were shown here for two mice in each group. (B) HuR staining in kidneys was increased in STZ-induced mice. Paraffin-embedded sections of kidneys from controls or STZ-induced mice were prepared and subjected to standard immuno-histochemistry staining for HuR (scale bar, 60  $\mu$ m). The intensities of HuR were quantified by Image J software, and 3 mice were quantified for each group. (C) HuR protein levels were increased in diabetic OVE26 mice as compared to control FVB mice. The kidney cortex from 3-month old OVE26 and control FVB mice were prepared and the expression of HuR was assessed by western blotting assay from these cortical lysates. (D) Nox4 RNA levels in the HuR IP complex were increased in diabetic mice, as compared to the ones in control animals. Kidney cortex lysates were prepared from control and STZ-induced mice, and immunoprecipitated by the HuR antibody. Then the presence of Nox4 mRNA in these IP complexes was assessed by RT-PCR (upper panel). Histogram showed the quantification against the trace amount presented in the total IgG complex (bottom panel). (E) Representative images showed HuR and Nox4 staining in paraffin embedded sections from healthy human and DN patients (scale bar, 60  $\mu$ m). (F) The intensities of HuR and Nox4 staining were quantified by Image J and normalized to the lowest expression level sample. The plot showed the positive correlation between HuR (x-axis) and Nox4 staining (y-axis). All data are presented as the mean  $\pm$  S.E of three repeats. \*,  $p < 0.05$ ; \*\*,  $p < 0.01$  in comparison with control or as indicated. The Student's *t*-test was used to compare two groups; and one-way ANOVA was used for comparison between multiple groups.

staining was strongly correlated with the levels of Nox4 ( $R = 0.8879$ , Figure 4F). In the diabetic animal models, we also confirmed that both HuR and Nox4 showed significantly increased levels, and co-localized in glomeruli (Supplementary Figure 5). Taken together, these data

demonstrate that HuR protein is able to regulate Nox4 protein translations in diabetic animals by increasing the binding affinity of HuR to Nox4 mRNA. Enhanced levels of HuR protein have been observed in patients with DN, suggesting a critical role of HuR in determining DN.



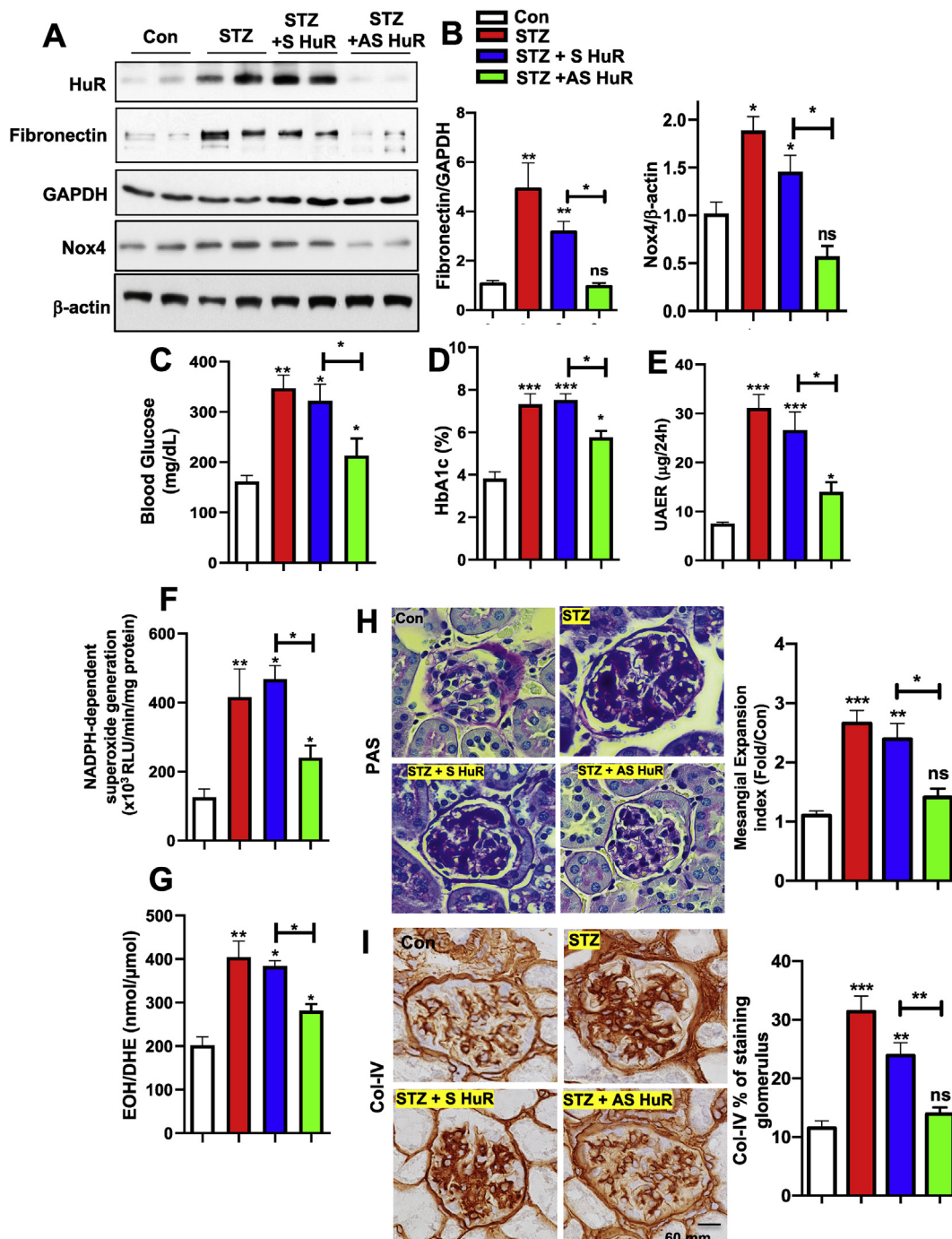


**Figure 5:** Inhibition of HuR protein in diabetic animals ameliorates matrix protein accumulation, renal function and histopathology. The expression of HuR, Nox4 and fibronectin (A) was assessed by western blotting assay in kidney cortical lysates from control, STZ-induced, STZ + sense (S) RNA against HuR, and STZ + antisense (AS) RNA against HuR mice. GAPDH and β-actin were used as loading controls. Band intensities were quantified by Image J, normalized to loading controls, and presented in B. (C–G), hyperglycemia, renal function and ROS were improved after HuR antisense treatment. Blood glucose (C) and HbA1c ratio (D) were measured in all groups. Renal function was assessed by measuring protein albumin levels in 24 h of urea collection. ROS levels were present as the levels of superoxides, measured by lucigenin chemiluminescence (F) and HPLC analysis (G). Representative PAS staining (H) and collagen type IV (Col-IV) (I) in kidney sections from the above four groups were shown here (scale bar, 60 μm). Pixel intensities were quantified by Image J, normalized to control samples, and present in H and I for PAS staining and Col-IV, respectively. Histograms represented the mean ± S.E of three to five mice in one group. \*,  $p < 0.05$ ; \*\*,  $p < 0.01$ , ns for non-significant, in comparison with control or as indicated. One-way ANOVA was used for comparison between multiple groups.

Next, we sought to explore the possibility of inhibiting HuR protein abundance to prevent the pathogenesis progress of type-1 diabetes in our mouse models. The inhibition of HuR protein expression by small interfering RNA (siRNAs, antisense RNA) was first described by

Sengupta et al. [19]. Antisense (AS) and sense (S) HuR was administered subcutaneously (90 ng/g body weight/day) after 10 weeks of STZ induction in type-1 diabetes in mice with ALZET osmotic pumps for a continuous 2 weeks. Similar strategies were previously reported

in our group for successfully inhibiting Nox4 in mice [9,13,20]. The measurement of HuR protein levels in the kidney cortex from experimental mice showed a significant reduction from STZ-induced increasing levels. Importantly, the levels of FN were sufficiently reduced in the STZ + AS HuR group (Figure 5A and B for quantification data), suggesting that MCs fibrotic injury was suppressed following the suppression of HuR protein expression. Furthermore, morphological changes in diabetic mouse kidneys have been carefully examined in the context of renal histopathology. Periodic acid–Schiff (PAS) staining showed glomerular surface area with mesangial matrix expansion was significantly increased in STZ-treated mice compared with controls, which was reduced in STZ-treated mice with AS HuR administration, but not S-HuR (Figure 5C and D for quantification). We also observed enhanced staining of Collagen IV in the glomeruli of STZ-treated mouse kidneys compared with control animals; however, such staining was suppressed in AS-HuR administrated STZ-induced animals. All images were quantified using the Image-J software (Figure 5E and F for quantification). Taken together, our data show that suppressing HuR by antisense oligonucleotides reduces severe renal pathogenesis progression in type-1 diabetic animals. These observations uncover an important role of targeting HuR protein as a potential therapeutic target for treating DN patients.

#### 4. DISCUSSION

We have previously shown that Nox4 deficiency or inhibition protects against renal injury and diabetic nephropathy in rodents [20,21]; however, the regulatory mechanism of Nox4 expression under these pathophysiological conditions has not yet been fully elucidated. In the present study, we demonstrate the crucial role of HuR in hyperglycemia-induced Nox4 up-regulation and matrix protein

accumulation during mesangial cell hypertrophy. HG triggers HuR cytoplasmic accumulation and promotes the binding between HuR and Nox4 mRNA. After binding to HuR through 3'-UTR AU rich elements, Nox4 mRNA stability is enhanced and Nox4 protein expression is up-regulated. Matrix protein accumulation is induced as characterized by the increased levels of fibronectin and  $\alpha$ -SMA. Finally, we also uncovered a similar mechanism in rodent kidney tissues, in which binding between HuR and Nox4 mRNA was enhanced in diabetic rodents as compared to control groups. More importantly, elevated protein levels of both HuR and Nox4 were observed and positively correlated in kidney sections from DN patients. Therefore we conclusively demonstrated for the first time that HuR acts as a critical post-transcriptional regulator of Nox4 expression in DN.

RNA-binding proteins have recently been identified to be crucial in both physiology and pathological conditions, as they are key components for the post-transcriptional regulation of gene expression [22]. A number of RNA-binding proteins have been characterized, including ELAV protein family members such as HuR, AU-rich binding factor, which is ubiquitously expressed and stabilizes mRNA by binding to their ARE-containing 3'-UTR. Emerging evidence has shown that HuR is involved in many essential physiological events, such as cancer and metabolic regulations [23,24]. In the kidney, HuR protein has been shown to contribute to ischemia, renal fibrosis, matrix protein accumulation and angiogenesis [25–27]. HuR is normally localized to the nucleus; however, in response to certain stress conditions, HuR is translocated to the cytoplasm and promotes the stability of the ARE-containing mRNAs. One of the most important findings in our current study is the upregulation and nuclei-to-cytoplasm translocation of HuR in mesangial cells upon HG stimulation. Such upregulation of HuR is also found in patients with DN, indicating the contribution of HuR to the pathogenesis of DN.

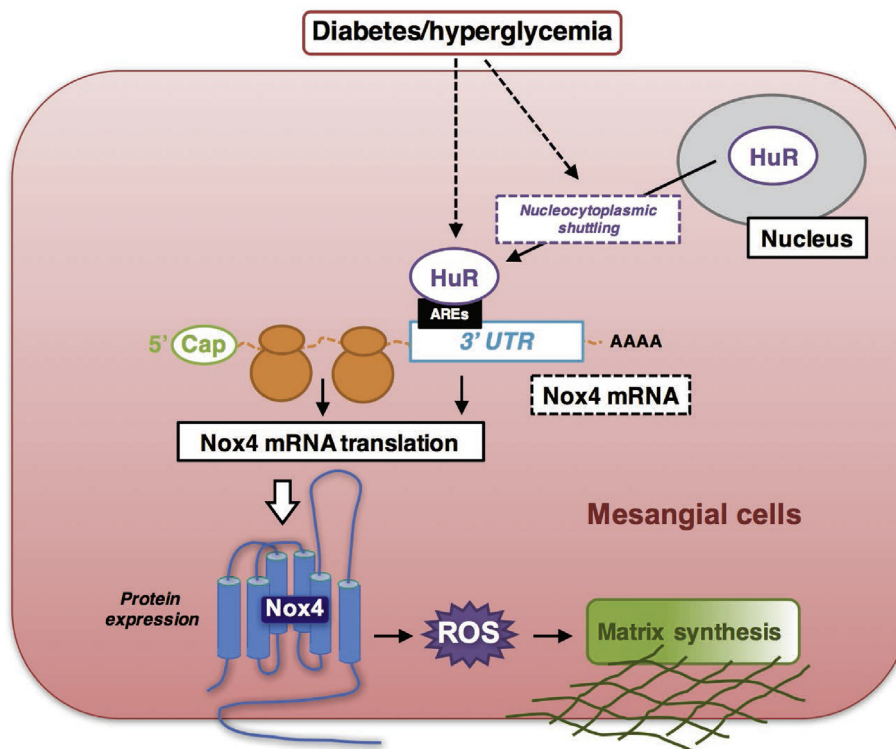


**Figure 6:** Schematic model of HuR/Nox4 interactions in diabetic nephropathy. Under hyperglycemia in diabetic kidney disease, molecular interactions between HuR protein and Nox4 3'-UTR are enhanced, which contributes to increased Nox4 protein expression and enhanced ROS generation, glomerular hypertrophy, and mesangial expansion.

Although it is known that Nox4 mRNA from various species bear long 3'-UTRs with several AREs, the mechanism involved in the post-transcriptional regulation of Nox4 is barely understood. As Nox4 and HuR showed a positive correlation, we postulated that HuR might regulate Nox4 expression by binding to its mRNA 3'-UTR. Through RNA EMSA and mutagenesis studies, we observed a profound and persistent residues-dependent HuR binding to Nox4 3'-UTR ARE regions. To our knowledge, this is the first study demonstrating that Nox4 mRNA is a target of the mRNA-stabilizing HuR protein. Other NADPH oxidase family proteins, such as Nox1 and Nox2, have also been indicated in diabetic kidney disease [28,29], showing that both the mRNA and protein levels were altered in DKD. However, Nox4 mRNA levels were not altered in diabetic mouse models ([13], GEO dataset GDS3990 and current studies), or in patients with diabetes (data from the Nephroseq website [30]). In addition, we have not detected the specific binding region of HuR on the promoter region of Nox2, nor Nox1. Therefore the regulation of Nox4 vs. Nox2/1 must be very different in responding to hyperglycemia.

Mechanistically, HuR nuclei-cytoplasm shuttling is a target of multiple signaling pathways, including the Mitogen-activated protein kinases and various members of the protein kinase C family, both of which can be regulated by ROS [31,32]. Moreover, recent studies have indicated that the activation of the immune system due to disturbances in the redox state of cells seems to contribute to renal damage and have demonstrated that ROS generated by NADPH oxidases are critical to oxidative stress in the kidney [7,33]. Our group and others have consistently shown that Nox4, an NADPH oxidase isoform predominantly expressed in kidney, is up-regulated in various renal cells upon the stimulation of HG and in kidneys from type-1 diabetes models [13,16,21,34]. Depletion of Nox4 leads to renal protection from glomerular injury in both STZ-induced diabetic and *ApoE* knockout mice [9,35]. It is important to note that Nox2 knockout mice did reveal a similar degree of diabetic renal injury as compared to the control groups [36], which is most likely due to the compensatory up-regulation of Nox4 at both the glomerular and cortical levels. Therefore considering the contribution of Nox4 in the kidney, Nox4 has remained the major target for manipulating renal ROS production *in vitro* and *in vivo*. Our studies here extend the regulatory mechanism to the epigenetic studies, and we discovered that the RNA binding protein, HuR, regulates Nox4 mRNA stability through translational controls of Nox4. In STZ-induced diabetic mouse or rat models, HuR was found to be up-regulated and bound to Nox4 3'-UTR stronger than in the control mice. Our results imply that the disruption of HuR–Nox4 mRNA binding has therapeutic potential for diabetic kidney disease. Although the outcomes from our studies in a mouse model of diabetes may not directly apply to diabetic patients, the findings provide new evidence for a better understanding of the biological activities of HuR in association with Nox4 in DN. The interaction between HuR and Nox4 might also be informative in other kidney cells, as Nox4 expressed in all major kidney cells, such as proximal tubular cells, podocytes, and endothelial cells, which suggests that HuR might also be universally expressed in all cell types. Given the important role that HuR plays in various cancer models, we are also expecting that such an interaction could be a potential target for developing further mechanistic studies. In treating DN, various PKC isoforms have been proposed to play important roles in the pathogenesis of diabetic nephropathies, such as PKC $\alpha$ , PKC $\beta$  [37]. Animals lacking both isoforms showed much improved reno-protective pathology after 8 weeks of diabetes, including glomerular hypertrophy, TGF- $\beta$ , and extracellular matrix. However, albuminuria was not entirely prevented in the double knockout mice compared to the single KO controls [38]. So far,

researchers have identified various mechanisms that different PKC isoforms play in promoting DN [37]. The inhibition of one or two of isoforms does not completely prevent the renal pathogenesis of DN, especial in diabetic patients; pan-inhibitor of PKC is also problematic due to its wide spectrum, which underlies the difficulty in identifying the suitable inhibitor for human clinical trials. A high dose of PKC inhibitors will commonly lead to increased mortality, as PKC isoforms are involved in so many essential cellular pathways, highlighting a fundamental difference between rodents and humans (another similar case would be antioxidants, see review [39]). Notably, small-molecule inhibitors against HuR, a downstream effector of PKC [40], have been a hotspot line for treating various cancers, especially in non-small cell lung cancer [41,42]. It has been widely accepted that the levels of HuR protein get elevated in many disease models, such as diabetes and various cancer types. In diabetes, the depletion of HuR greatly diminished retinal pathology in diabetic animals [43]. In the kidney, the increase in HuR protein levels leads to the stabilization of mRNA levels of *CTGF*, *TGF $\beta$ 1*, *FOS* and *SNAIL*, contributing to EMT and diabetic nephropathy [10]. Together, the previous studies strongly suggested a critical role for HuR up-regulation in the development of diabetic complications. Here, we utilized a small RNAi technology to suppress HuR protein expression *in vivo* by implanting mice with an osmotic pump for a continuous two-week period of time. The expression of HuR in these animals with antisense oligo RNA against HuR remained undetectable, even in the STZ-induced diabetic animals; however, in the animals with sense oligo, the expression of HuR was sustained at higher levels. Meanwhile, we observed greater reduction of fibronectin protein levels, suggesting an improvement in renal matrix protein accumulation with improvements in renal pathology. Most importantly, HuR inhibition attenuated the severity of structural abnormalities, as shown by the reduction in glomerular hypertrophy, collagen type IV expression, and mesangial expansion. Overall, our data provide compelling evidence for a beneficial effect of inhibiting HuR in the mouse model of DN. Importantly, our study suggests that a relatively short-term treatment can be effective even when initiated in mice with established diabetes and diabetic kidney disease.

In conclusion, the current study for the first time provides the direct evidence that HuR is a critical component of a signal transduction pathway that links renal injury to hyperglycemia-mediated pathogenesis response in DN. We further confirm that HG-enhanced Nox4 expression and mRNA stability are mediated by RNA binding protein, HuR. The up-regulation of Nox4 was not only dependent on the up-regulation of HuR, but also on the nuclear-cytoplasmic shuttling of HuR (working model Figure 6). Even though we are employing only type-1 diabetic mouse/rat models in this study, we are not ruling out the possible similar mechanism of HuR–Nox4 interaction in type-2 diabetic models. *In vitro*, high glucose treatments represent some common mechanisms that are shared in both type-1 and type-2 diabetes. Others have also reported that mRNA and protein levels of Nox4 increased significantly in type-2 diabetic mouse/rat models, such as db/db mice [33]; therefore, we are expecting a similar role of HuR–Nox4 interaction in type-2 diabetic models. Such a mechanism warrants further study, which is of great importance for developing additional therapeutic options that might be utilized for treating DN in patients with either type-1 or type-2 diabetes.

## ACKNOWLEDGMENTS

This work is dedicated to Dr. Yves Gorin and Dr. Hanna Abboud, both of whom passed away recently. They initiated and supervised the project in its early stages, and their mentorship is gratefully acknowledged. QS is supported by the JDRF

Advanced Postdoctoral Fellowship (3-APF-2016-205-A-N) and the JDRF transition award (1-FAC-2019-858-A-N). HEA and YG were supported by NIH grant DK 33665. MAB is supported by the Zachry Foundation endowment.

## APPENDIX A. SUPPLEMENTARY DATA

Supplementary data to this article can be found online at <https://doi.org/10.1016/j.molmet.2020.02.011>.

## CONTRIBUTIONS

QS designed, conducted the experiments, analyzed the data and wrote the manuscripts. DYL and DF conducted experiments. HEA, MAB and YG designed the experiments and contributed to the discussion of the results. MAB edited the manuscripts.

## CONFLICT OF INTEREST

The authors declare no competing financial interests.

## REFERENCES

- Rosen, E.D., Kaestner, K.H., Natarajan, R., Patti, M.E., Sallari, R., Sander, M., et al., 2018. Epigenetics and epigenomics: implications for diabetes and obesity. *Diabetes* 67(10):1923–1931.
- Cho, N.H., Shaw, J.E., Karuranga, S., Huang, Y., da Rocha Fernandes, J.D., Ohlrogge, A.W., et al., 2018. IDF Diabetes Atlas: global estimates of diabetes prevalence for 2017 and projections for 2045. *Diabetes Research and Clinical Practice* 138:271–281.
- Kato, M., Natarajan, R., 2019. Epigenetics and epigenomics in diabetic kidney disease and metabolic memory. *Nature Reviews Nephrology* 15(6):327–345.
- Anders, H.J., Huber, T.B., Isermann, B., Schiffer, M., 2018. CKD in diabetes: diabetic kidney disease versus nondiabetic kidney disease. *Nature Reviews Nephrology* 14(6):361–377.
- Kashihara, N., Haruna, Y., Kondeti, V.K., Kanwar, Y.S., 2010. Oxidative stress in diabetic nephropathy. *Current Medicinal Chemistry* 17(34):4256–4269.
- Pan, H.Z., Zhang, L., Guo, M.Y., Sui, H., Li, H., Wu, W.H., et al., 2010. The oxidative stress status in diabetes mellitus and diabetic nephropathy. *Acta Diabetologica* 47(Suppl. 1):71–76.
- Gorin, Y., Block, K., 2013. Nox4 and diabetic nephropathy: with a friend like this, who needs enemies? *Free Radical Biology and Medicine* 61:130–142.
- Bedard, K., Krause, K.H., 2007. The NOX family of ROS-generating NADPH oxidases: physiology and pathophysiology. *Physiological Reviews* 87(1):245–313.
- Eid, A.A., Lee, D.Y., Roman, L.J., Khazim, K., Gorin, Y., 2013. Sestrin 2 and AMPK connect hyperglycemia to Nox4-dependent endothelial nitric oxide synthase uncoupling and matrix protein expression. *Molecular and Cellular Biology* 33(17):3439–3460.
- Yu, C., Xin, W., Zhen, J., Liu, Y., Javed, A., Wang, R., et al., 2015. Human antigen R mediated post-transcriptional regulation of epithelial–mesenchymal transition related genes in diabetic nephropathy. *Journal of Diabetes* 7(4):562–572.
- Gorin, Y., Ricono, J.M., Wagner, B., Kim, N.H., Bhandari, B., Choudhury, G.G., et al., 2004. Angiotensin II-induced ERK1/ERK2 activation and protein synthesis are redox-dependent in glomerular mesangial cells. *Biochemical Journal* 381(Pt 1):231–239.
- Sataranatarajan, K., Feliars, D., Mariappan, M.M., Lee, H.J., Lee, M.J., Day, R.T., et al., 2012. Molecular events in matrix protein metabolism in the aging kidney. *Aging Cell* 11(6):1065–1073.
- Shi, Q., Viswanadhapalli, S., Friedrichs, W.E., Velagapudi, C., Szyndralewicz, C., Bansal, S., et al., 2018. Nox4 is a target for Tuberin deficiency syndrome. *Scientific Reports* 8(1):3781.
- Zhao, Q.D., Viswanadhapalli, S., Williams, P., Shi, Q., Tan, C., Yi, X., et al., 2015. NADPH oxidase 4 induces cardiac fibrosis and hypertrophy through activating Akt/mTOR and NFκB signaling pathways. *Circulation* 131(7):643–655.
- Khazim, K., Gorin, Y., Cavaglieri, R.C., Abboud, H.E., Fanti, P., 2013. The antioxidant silybin prevents high glucose-induced oxidative stress and podocyte injury in vitro and in vivo. *American Journal of Physiology. Renal Physiology* 305(5):F691–F700.
- Gorin, Y., Cavaglieri, R.C., Khazim, K., Lee, D.Y., Bruno, F., Thakur, S., et al., 2015. Targeting NADPH oxidase with a novel dual Nox1/Nox4 inhibitor attenuates renal pathology in type 1 diabetes. *American Journal of Physiology. Renal Physiology* 308(11):F1276–F1287.
- Nayak, B.K., Shanmugasundaram, K., Friedrichs, W.E., Cavaglieri, R.C., Patel, M., Barnes, J., et al., 2016. HIF-1 mediates renal fibrosis in OVE26 type 1 diabetic mice. *Diabetes* 65(5):1387–1397.
- Fonseca, B.D., Smith, E.M., Yelle, N., Alain, T., Bushell, M., Pause, A., 2014. The ever-evolving role of mTOR in translation. *Seminars in Cell & Developmental Biology* 36:102–112.
- Sengupta, S., Jang, B.C., Wu, M.T., Paik, J.H., Furneaux, H., Hla, T., 2003. The RNA-binding protein HuR regulates the expression of cyclooxygenase-2. *Journal of Biological Chemistry* 278(27):25227–25233.
- Gorin, Y., Block, K., Hernandez, J., Bhandari, B., Wagner, B., Barnes, J.L., et al., 2005. Nox4 NAD(P)H oxidase mediates hypertrophy and fibronectin expression in the diabetic kidney. *Journal of Biological Chemistry* 280(47):39616–39626.
- Lee, D.Y., Wauquier, F., Eid, A.A., Roman, L.J., Ghosh-Choudhury, G., Khazim, K., et al., 2013. Nox4 NADPH oxidase mediates peroxynitrite-dependent uncoupling of endothelial nitric-oxide synthase and fibronectin expression in response to angiotensin II: role of mitochondrial reactive oxygen species. *Journal of Biological Chemistry* 288(40):28668–28686.
- Hentze, M.W., Castello, A., Schwarzl, T., Preiss, T., 2018. A brave new world of RNA-binding proteins. *Nature Reviews Molecular Cell Biology* 19(5):327–341.
- Rajasingh, J., 2015. The many facets of RNA-binding protein HuR. *Trends in Cardiovascular Medicine* 25(8):684–686.
- Srikantan, S., Gorospe, M., 2012. HuR function in disease. *Frontiers in Bioscience* 17:189–205.
- Shang, J., Zhao, Z., 2017. Emerging role of HuR in inflammatory response in kidney diseases. *Acta Biochimica et Biophysica Sinica* 49(9):753–763.
- Gummadi, L., Taylor, L., Curthoys, N.P., 2012. Concurrent binding and modifications of AUF1 and HuR mediate the pH-responsive stabilization of phosphoenolpyruvate carboxykinase mRNA in kidney cells. *American Journal of Physiology. Renal Physiology* 303(11):F1545–F1554.
- Ayupova, D.A., Singh, M., Leonard, E.C., Basile, D.P., Lee, B.S., 2009. Expression of the RNA-stabilizing protein HuR in ischemia-reperfusion injury of rat kidney. *American Journal of Physiology. Renal Physiology* 297(1):F95–F105.
- Oudit, G.Y., Liu, G.C., Zhong, J., Basu, R., Chow, F.L., Zhou, J., et al., 2010. Human recombinant ACE2 reduces the progression of diabetic nephropathy. *Diabetes* 59(2):529–538.
- Fukuda, M., Nakamura, T., Kataoka, K., Nako, H., Tokutomi, Y., Dong, Y.F., et al., 2010. Potentiation by candesartan of protective effects of pioglitazone against type 2 diabetic cardiovascular and renal complications in obese mice. *Journal of Hypertension* 28(2):340–352.
- Woroniecka, K.I., Park, A.S., Mohtat, D., Thomas, D.B., Pullman, J.M., Susztak, K., 2011. Transcriptome analysis of human diabetic kidney disease. *Diabetes* 60(9):2354–2369.
- Gama-Carvalho, M., Carmo-Fonseca, M., 2001. The rules and roles of nucleocytoplasmic shuttling proteins. *FEBS Letters* 498(2–3):157–163.
- Kodiha, M., Stochaj, U., 2012. Nuclear transport: a switch for the oxidative stress-signaling circuit? *Journal of Signal Transduction* 2012:208650.

- [33] Sedeek, M., Nasrallah, R., Touyz, R.M., Hebert, R.L., 2013. NADPH oxidases, reactive oxygen species, and the kidney: friend and foe. *Journal of the American Society of Nephrology* 24(10):1512–1518.
- [34] Gorin, Y., Wauquier, F., 2015. Upstream regulators and downstream effectors of NADPH oxidases as novel therapeutic targets for diabetic kidney disease. *Molecules and Cells* 38(4):285–296.
- [35] Jha, J.C., Gray, S.P., Barit, D., Okabe, J., El-Osta, A., Namikoshi, T., et al., 2014. Genetic targeting or pharmacologic inhibition of NADPH oxidase nox4 provides renoprotection in long-term diabetic nephropathy. *Journal of the American Society of Nephrology* 25(6):1237–1254.
- [36] You, Y.H., Okada, S., Ly, S., Jandeleit-Dahm, K., Barit, D., Namikoshi, T., et al., 2013. Role of Nox2 in diabetic kidney disease. *American Journal of Physiology. Renal Physiology* 304(7):F840–F848.
- [37] Teng, B., Duong, M., Tossidou, I., Yu, X., Schiffer, M., 2014. Role of protein kinase C in podocytes and development of glomerular damage in diabetic nephropathy. *Frontiers in Endocrinology* 5:179.
- [38] Meier, M., Park, J.K., Overheu, D., Kirsch, T., Lindschau, C., Gueler, F., et al., 2007. Deletion of protein kinase C-beta isoform in vivo reduces renal hypertrophy but not albuminuria in the streptozotocin-induced diabetic mouse model. *Diabetes* 56(2):346–354.
- [39] Tavafi, M., 2013. Diabetic nephropathy and antioxidants. *Journal of Nephropathology* 2(1):20–27.
- [40] Nutter, C.A., Kuyumcu-Martinez, M.N., 2018. Emerging roles of RNA-binding proteins in diabetes and their therapeutic potential in diabetic complications. *Wiley Interdisciplinary Reviews. RNA* 9(2).
- [41] Muralidharan, R., Mehta, M., Ahmed, R., Roy, S., Xu, L., Aube, J., et al., 2017. HuR-targeted small molecule inhibitor exhibits cytotoxicity towards human lung cancer cells. *Scientific Reports* 7(1):9694.
- [42] Lang, M., Berry, D., Passecker, K., Mesteri, I., Bhujju, S., Ebner, F., et al., 2017. HuR small-molecule inhibitor elicits differential effects in adenomatous polyposis and colorectal carcinogenesis. *Cancer Research* 77(9):2424–2438.
- [43] Amadio, M., Pascale, A., Cupri, S., Pignatello, R., Osera, C., D Agata, V., et al., 2016. Nanosystems based on siRNA silencing HuR expression counteract diabetic retinopathy in rat. *Pharmacological Research* 111:713–720.